Synthesis of 1,6/7-$(NO_2)_2$Perylenediimide and 1,6/7-$(NH_2)_2$Perylenediimide: Regioisomerically Pure Materials for Organic Electronics

Adèle Gapin,[†,a] Arthur H. G. David,[†,a] Magali Allain,[a] Dorian Masson,[a] Olivier Alévêque,[a] Thomas Ave,[a] Laura Le Bras,*[,b] Piétrick Hudhomme*[,a] and Antoine Goujon*[,a]

[a] Univ Angers, CNRS, MOLTECH-Anjou, SFR MATRIX, F- 49000 Angers, France

[b] Laboratoire Chrono-environnement (UMR 6249), Université de Franche-Comté, 16 route de Gray, 25030 Besançon, France

antoine.goujon@univ-angers.fr

[†] These two authors contributed equally

The use of perylenediimide (PDI) building blocks in materials for organic electronic is of considerable interest. The introduction of peripheral groups in their *ortho* and *bay* positions radically modify their optoelectronic properties. In this article, we describe an efficient method to afford regioisomerically pure 1,6/7-$(NO_2)_2$- and $(NH_2)_2$-PDIs employing two key steps: the selective crystallization of 1,6-$(NO_2)_2$-perylene-3,4,9,10-tetracarboxy tetrabutylester and the nitration of regiopure 1,7-Br_2-PDI with silver nitrite. The optoelectronic properties of the resulting regioisomerically pure dinitro, diamino-PDIs and bisazacoronenediimides (BACDs) are reported and demonstrate the need to separate both regioisomers of such n-type organic semiconductors for their inclusion in advanced optoelectronic devices.

Introduction

Perylenediimide (PDI) based materials have been increasingly drawing attention in organic electronics.[1] Their high electron-affinity and strong visible-light absorption combined with the high electron-mobilities measured in thin films make them attractive n-type organic semiconductors.[2] They can be found in a variety of organic electronics devices as active materials such as Organic Solar Cells (OSCs) as Non-Fullerene-Acceptors (NFA)[3,4] or Electron Transporting Layer[5] for example and they are rising in chiral optoelectronics applications.[6] The choice of imide side-chain usually controls their self-assembly and solubility, while the modification of their *ortho* and *bay* positions drastically change their optical and electronic properties: in consequence, an intense synthetic work has been made to introduce various chemical functionalities and extend/dope their aromatic core.[7] The most popular and widespread strategy to functionalize the *bay* position is to first perform an halogenation. The brominated PDIs can be engaged in palladium-catalysed cross-coupling reactions or nucleophilic aromatic substitutions among others. The use of a large excess of bromine allows for the preparation of Br_2PDI, an essential starting material of conjugated polymers[8] or core-extended polyaromatic hydrocarbons diimides.[9] However, preparing this important intermediate of PDI chemistry results in a mixture of 1,6-Br_2PDI and 1,7-Br_2PDI regioisomers which cannot be separated. In some cases the regioisomers can be separated and isolated later on after several synthetic steps,[10] but this is not generalizable to all 1,6/7 mixtures. Jager and collaborators reported a strategy to prepare regioisomerically pure 1,7-Br_2PDI starting from the preparation of perylene-3,4,9,10-tetracarboxy tetrabutylester (PTE).[11] After bromination, the 1,7 regioisomer can be separated and obtained

pure on the multi-gram scale by successive crystallizations. 1,7-Br_2PTE can then be converted into the desired 1,7-Br_2PDI in two efficient steps. However, there are no method giving access to pure 1,6-Br_2PDI. Very recently, the groups of Wu and Xia reported how to prepare 1,6-$(OTf)_2$PDI starting from a tetrabrominated perylenemonoimide after 4 additional synthetic steps.[12] This route allows the preparation of a derivative of analogous reactivity to its halogenated counterpart, which can be engaged into Pd-catalysed cross-coupling reactions. However, it requires a significant synthetic work, including a Pd-catalysed imide formation involving the use of hazardous carbon monoxide. Nevertheless, this work and all effort directed toward the study of regiopure material is justified. PDI regioisomers have noticeably different optical and electronic properties, in addition to having different solid-state packing, which greatly affect their effective frontiers orbital energy levels and charge diffusion ability in thin films. These differences can greatly affect the performances and properties of organic electronic devices.[13,14]

Recently, nitrated PDIs or NO_2PDIs have demonstrated their potential as an alternative to BrPDI: they are prepared faster in high yield and selectivity and require little purification effort.[15] Moreover, NO_2PDIs appear more versatile than their halogenated equivalents. Not only they can be engaged in nucleophilic aromatic substitutions, hetero-annulation reactions with atoms such as oxygen, sulphur, selenium and nitrogen, and their use as electrophile in Pd-catalysed cross-coupling reactions has been recently demonstrated.[16–18] Moreover, they can be reduced into NH_2PDI, a material precursor of AzaBenzannulated PDIs and BisAzaCoroneneDiimides (BACDs), when using $(NH_2)_2$PDI)[19–21] which both recently showed promising results as active n-type semiconductors,[22,23] fluorescent probes[24] and NFAs in OSCs.[25] Therefore, the development of synthetic pathways to efficiently prepare regioisomerically pure 1,6/7-$(NO_2)_2$PDIs and 1,6/7-$(NH_2)_2$PDIs is more relevant than ever. Studies report the use of pure 1,7-$(NO_2)_2$PDIs and 1,7-$(NH_2)_2$PDIs regioisomers, stating that they were obtained by successive crystallization.[23,24,26–28] However, the solvent used to do so has not been reported and the efficiency of this kind of purification is dependent on the nature of the imide chains used. Another work reports the use of pure 1,6/7-$(NO_2)_2$PDIs and their subsequent reduction.[29] The pure nitrated regioisomers were separated by high-performance liquid-chromatography, a technique limiting the scale of material obtained and that is again dependant on the nature of the imide chains.

Herein, we report a method that can afford regiopure materials on the multigram scale and allows us to introduce an imide chain of choice. This can be achieved *via* nitration or bromination of PTE. The key steps are the isolation of pure 1,6-$(NO_2)_2$PTE by precipitation confirmed by single crystal X-ray diffraction, and the efficient nitration of 1,7-Br_2PDI by treatment with silver nitrite.

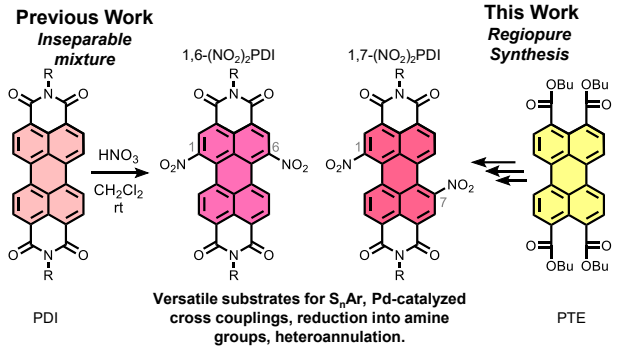

Fig. 1 Conventional non-regioselective preparation of 1,6/7-$(NO_2)_2$PDIs by treatment with fuming nitric acid and the regiopure pathway starting from PTE.

Results and Discussion

PTE **1** was prepared and nitrated following procedures from the literature[30] to afford a 55:45 mixture of 1,6/7-$(NO_2)_2$PTE **2** (**Figure 2a**). We attempted to apply the same crystallisation conditions that are reported to separate 1,7-Br_2PTE from 1,6-Br_2PTE.[11] Large needle-like orange crystals were formed and recovered by filtration. After a second crystallization, ^{1}H NMR confirmed that a single regioisomer was isolated (**Figure 2b**). The same results were obtained by performing two successive recrystallization in hot acetonitrile. The filtered crystals were suitable for X-ray diffraction, and their study allowed us to unambiguously determine that the isolated regioisomer was 1,6-$(NO_2)_2$PTE **1,6-2** (**Figure 2c, Figure S62**). The compound crystallizes in triclinic *P*-1 space group. The structure presents a twisted angle of 17.8° between the two naphthalene fragment of the perylene core, comparable to those observed for PDI analogues[17]. The molecules are stacked in a head to tail manner along the *a* axis of the unit cell with a distance of 3.53 Å and 3.56 Å between them (see **Figure S63**). Interestingly, the regioisomer obtained by successive precipitations of $(NO_2)_2$PTE here is the opposite one as in the case of Br_2PTE. It was obtained in a 39% yield compared to the initial mixture **2** containing 55% of **1,6-2**, which gives a 71% yield for the recrystallization. The dye **1,6-2** was further efficiently transformed into 1,6-$(NO_2)_2$perylenetetracarboxylic-dianhydride or 1,6-$(NO_2)_2$PTCDA **1,6-3** by the action of chlorosulfonic acid. This key intermediate can be reacted with any amine to afford regio-pure 1,6-$(NO_2)_2$PDIs **1,6-4** (**Figure 3a**) following a simple 4 steps sequence, starting from materials that can be prepared on tenth of grams scale in the laboratory following well-known procedures.

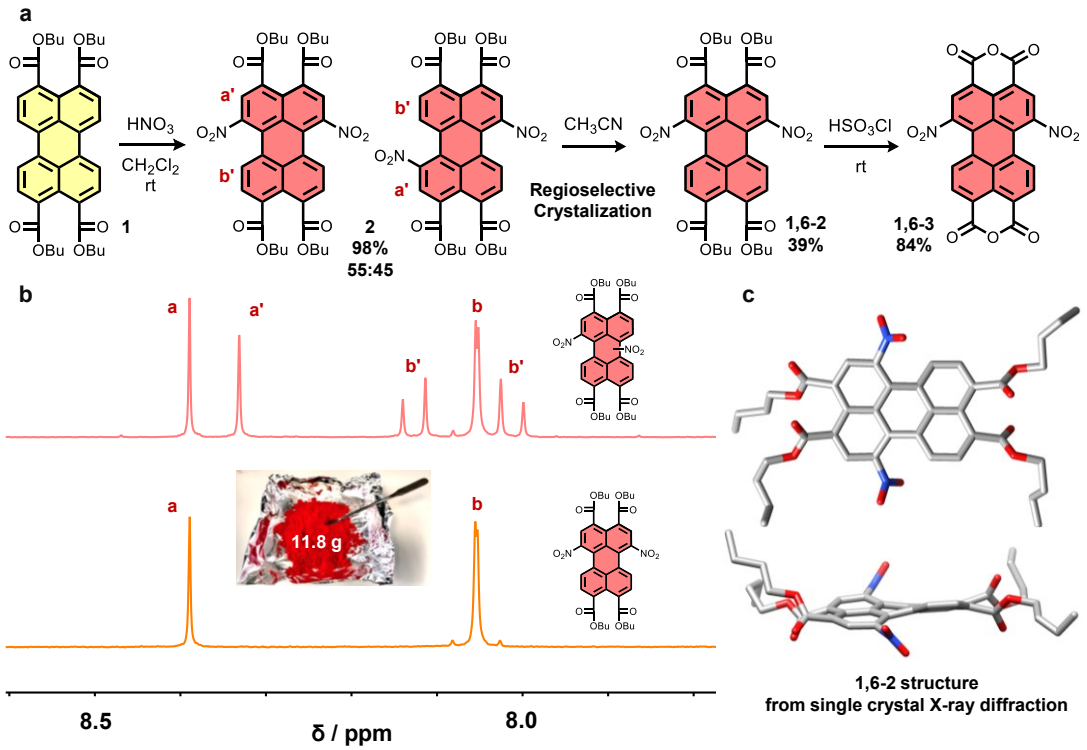

Fig. 2 a) Synthesis of regioisomerically pure 1,6-$(NO_2)_2$PTCDA **1,6-3**. b) Partial ^{1}H NMR in $CDCl_3$ (300 MHz) of the 55:45 mixture of 1,6/7-$(NO_2)_2$PTE **2** (top) and pure 1,6-$(NO_2)_2$PTE **1,6-2** (bottom) obtained after two crystallizations. c) Molecular structure of 1,6-$(NO_2)_2$PTE **1,6-2** obtained by single-crystal X-ray diffraction, from above and from the side, hydrogen atoms and solvent molecules omitted for clarity.

With one pure regioisomer in hands, we investigated how to turn 1,7-Br_2PTE into its nitrated equivalent 1,7-$(NO_2)_2$PTE. We prepared 1,7-Br_2PTE by following the method reported by Jager and collaborators.[11] Several reports describe how to substitute bromine by nitro groups *via* copper-catalysed reactions involving nitrite salts.[31–33] However, such reaction led to the decomposition of 1,7-Br_2PTE. Interestingly, the replacement of a bromine atom by a nitro group was reported on thiophene derivatives by the simple use of silver nitrate.[34] 1,7-Br_2PTE was refluxed in toluene in presence an excess of $AgNO_3$ which led to its very slow conversion into a mixture of mono nitrated species and decomposition products along with a small amount of targeted material. $AgNO_3$ was substituted by $AgNO_2$ hoping that it could lead to the target by simple S_NAr reaction. 1,7-Br_2PTE was refluxed in toluene in presence an excess of $AgNO_2$ and this time the targeted species 1,7-$(NO_2)_2$PTE was a formed along the mono nitrated derivate and a significant amount of remaining starting material. These encouraging results suggested that the reaction should performed better on the more reactive and electron-deficient 1,7-Br_2PDI **1,7-6**. Therefore, 1,7-Br_2PTCDA **1,7-5** was prepared and reacted with an amine to form 1,7-Br_2PDI **1,7-6**. This intermediate was reacted with $AgNO_2$ in toluene at reflux temperature in a pressured vial, which afforded the regiopure 1,7-$(NO_2)_2$PDI **1,7-4** with an excellent yield of 90% (**Figure 3a**). Interestingly, adjusting and lowering the amount of silver nitrite afforded the mono-substituted compound 1(Br)-7(NO_2)PDI **S1**, which could be an interesting intermediate for the preparation of dissymmetrical compounds (see Supporting Information, **Scheme S3**). ^{1}H NMR comparison of **1,6-4, 1,7-4**, and the mixture of regioisomers resulting from the direct nitration of a PDI bearing the same imide chains (see Supporting Information, **Scheme S5**) confirms that we developed an efficient synthetic pathway to prepare regiopure 1,6-$(NO_2)_2$PDI **1,6-4** and 1,7-$(NO_2)_2$PDI **1,7-4**.

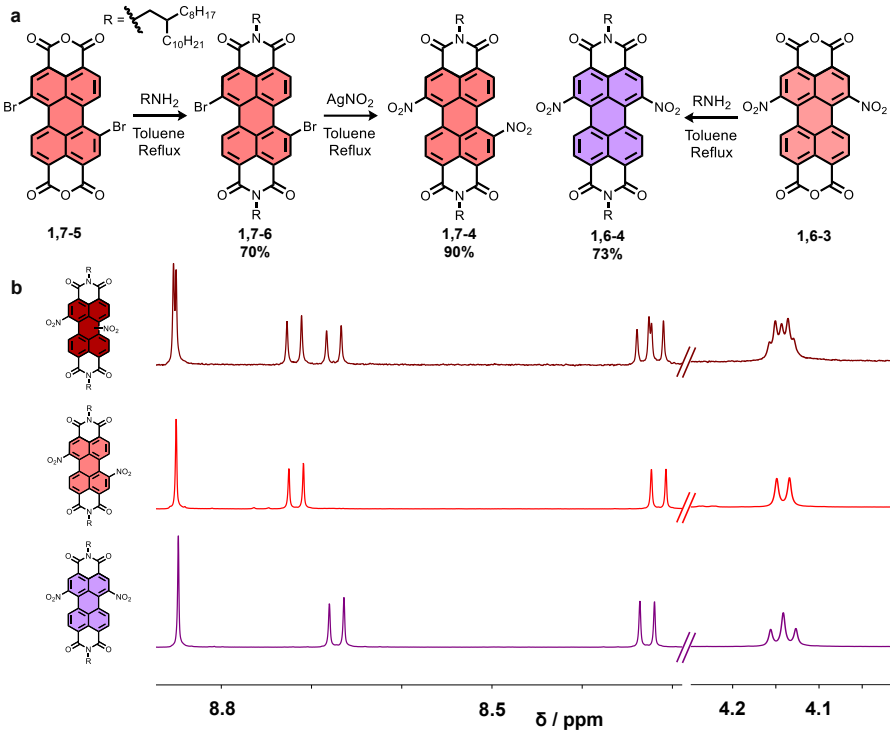

Fig 3. a) Synthesis of regioisomerically pure 1,7-$(NO_2)_2$PDI **1,7-4** and 1,6-$(NO_2)_2$PDI **1,6-4**. b) Partial ^{1}H NMR in $CDCl_3$ (500 MHz) of the 1:1 mixture of 1,6/7-$(NO_2)_2$PDI **4** (top), pure 1,6-$(NO_2)_2$PDI **1,6-4** (middle) and pure 1,7-$(NO_2)_2$PDI **1,7-4** (bottom).

We further reduced the nitro groups into amines to obtain pure 1,6-$(NH_2)_2$PDI **1,6-7** and 1,7-$(NH_2)_2$PDI **1,7-7** by reaction with hydrazine monohydrate in presence of Pd/C. The comparison of their ^{1}H NMR spectra to the regioisomeric mixture can be seen in **Figure S50** and confirms that there was no regioisomerization during this process. These dyes were further converted into BACD derivatives following a light-driven procedure recently reported by our group[35], which afforded the regiopure extended imide materials **1,6-8** and **1,7-8** in high yields. Again, no regioisomerization was observed (**Figure S51**). Analogous materials prepared from other aldehydes were reported as single 1,6/7 regioisomers before but at the cost on multiple tedious column chromatography performed on the mixture.[19]

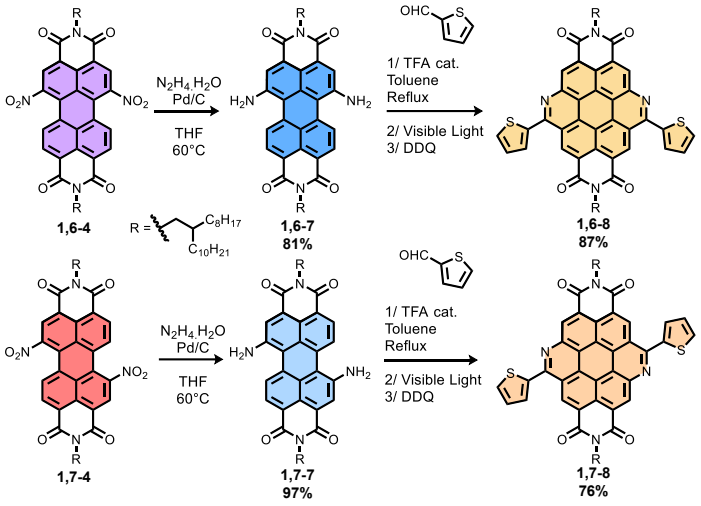

Fig. 4 Synthesis of regioisomerically pure 1,6-$(NH_2)_2$PDI **1,6-7** and 1,7-$(NH_2)_2$PDI **1,7-7** and corresponding BisAzaCoroneneDiimides **1,6-8** and **1,7-8**.

Interestingly, striking visual differences could be observed for dried samples of **1,6-4** and **1,7-4**. The 1,6 derivative displays a deep purple colour while the 1,7 one shows a vibrant red tone. Similarly, different shades of blue can be seen for the 1,6/7-$(NH_2)_2$PDI regioisomers **1,6-7** and **1,7-7**. At last, the two BACD derivatives **1,6-8** and **1,7-8** also display variations of orange colour. UV-visible spectroscopy measurements were performed to compare the photophysical properties of the regioisomers (**Figure 5**). The nitro derivative **1,6-4** shows a slightly red-shifted (520 nm) absorption maximum and a small shoulder at low energy compare to the **1,7-4** regioisomer (518 nm) as displayed in **Figure 5a**. In film, both regioisomers see their absorption maximum red-shifting and a narrower band at low energy (**Figure S4** and **S8**). Amine-functionalized derivatives also exhibit differences in absorption maximum: 587 nm for **1,6-7** and 616 nm for **1,7-7** (**Figure 5b**). Once again, in films lead to a red-shift of the absorption maximum in both case (**Figure S12** and **S16**), but in the case of the 1,6 regioisomer an inversion of the absorption ratio between the first and second shoulder of the first absorption band can be observed (**Figure S12**). At last, the thiophene-appended BACD derivatives absorbs light up to around 550 nm but they display a maximum at higher energy: at 389 nm for **1,6-8** and 373 nm for **1,7-8** (**Figure 5c**). Their processing in films red-shifts their absorption up to around 600 nm (**Figure S20** and **S24**) along with a noticeable loss of fine structure more pronounced for the 1,6 regioisomer than the 1,7 one. All the compounds showed high extinction ε in solution, with little differences depending of the regioisomers when it comes to the nitrated or amino derivatives. However, **1,6-8** absorbs light more strongly than **1,7-8** at high energy. These

dyes are poorly fluorescent (quantum yields between 0 and 5%, see **Table 1** and **S1** and **Figure 5a,b,c**). Overall the differences of optical properties for each regioisomers of the same compound and the variations observed when going from solutions to films in term of band position and shape strongly suggest different solid-state organization. **Figure 5d** illustrates these differences as seen with the naked eye.

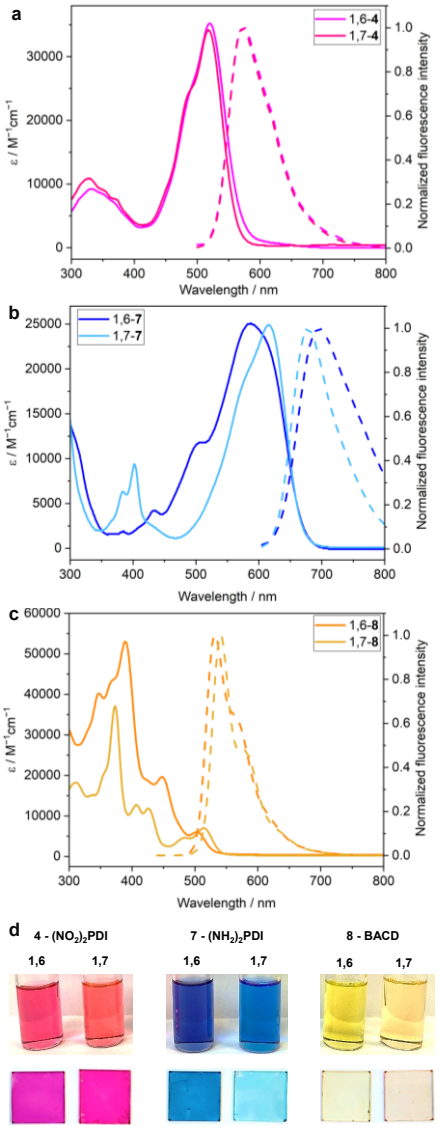

Fig. 5 Absorption (solid line) and normalized emission (dashed lines) spectra of the regioisomerically pure dyes **4** (**a**, λ_{exc} = 480 nm), **7** (**b**, λ_{exc} = 586 nm) recorded in CH_2Cl_2 and **8** (**c**, λ_{exc} = 387 nm) recorded in $CHCl_3$ at a concentration of *ca.* 1×10^{-5} M. **d**) Photograph of solution of the regioisomerically pure compounds **4**, **7** and **8** (top) and corresponding spin-coated thin films on glass substrates (bottom).

These studies were complemented by cyclic voltammetry, performed in a glovebox in CH_2Cl_2 (for **4** and **7**) and $CHCl_3$ (for **8**) with 0.1 M *n*-Bu_4NPF_6 (**Figure 6**). When scanning toward negative potentials, **1,6-4** and **1,7-4** reveals the expected two reduction waves typical of perylenediimides dyes. The 1,6 regioisomer can be reduced at a higher potential compared to the 1,7, making it a better electron acceptor. The amine-decorated compounds **1,6-7** and **1,7-7** show the same two reduction waves but can also be oxidized when scanning toward positive potentials. Two oxidation waves can be detected for **1,7-7** in the range studied, whereas only one for the **1,6-7** analogue. If both compounds can be reduced at similar potential, the **1,7-7** regioisomers is oxidized at a lower potential. When it comes to BACD derivatives, the first reduction is observed at -1.23 V for **1,6-8** and −1.14 V for **1,7-8** and the resulting HOMO and LUMO energy levels are analogous. Nevertheless, similarly to the case of the

spectroscopic studies, the electrochemical investigations presented here highlight the differences of electronic behavior and properties of each distinct regioisomer. The different optoelectronic properties of the different regioisomerically pure dyes are summarized in **Table 1**, which demonstrates and renders the separation of these regioisomers of key importance for their implementation in advanced optoelectronic devices.

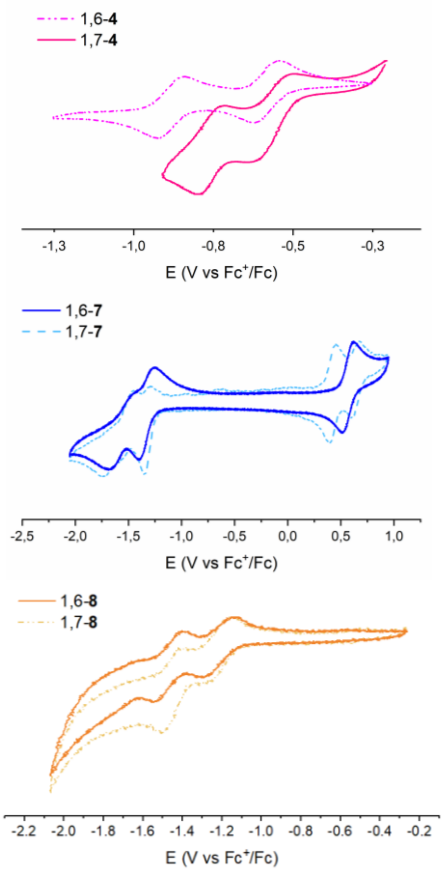

Fig. 6 Cyclic voltammetry of dyes **4**, **7** (in CH_2Cl_2), and **8** (in $CHCl_3$), scanned toward negative potentials, with *n*-Bu_4NPF_6 (0.1 M) as electrolyte.

Table 1 Summary of the optoelectronic properties of the regioisomerically pure dyes **4** and **7** in CH_2Cl_2 and **8** in $CHCl_3$.

Compound	λ_{abs} (nm)[a]	ε ($M^{-1}cm^{-1}$)[b]	λ_{em} (nm)	Φ_f (%)	E^{LUMO} (eV)	E_{calc}^{HOMO} (eV)	$\Delta E^{HOMO-LUMO}$ (eV)
1,6-4	520	4.0×10^4	576	0.062	−4.29	−6.37	2.08
1,7-4	518	4.0×10^4	572	1.1	−4.30	−6.47	2.17
1,6-7	587	2.7×10^4	696	N/A	−3.55	−5.17	1.62
1,7-7	616	2.8×10^4	678	N/A	−3.55	−5.13	1.58
1,6-8	389	5.9×10^4	532	4.9	−3.68	−5.75	2.07
1,7-8	373	4.4×10^4	541	4.0	−3.67	−5.74	2.07

[a]Maximum wavelength of the strongest energy absorption band given for the spectrum in solution. [b]Extinction coefficient of the strongest energy absorption band.

To gain deeper insights into the photophysical behavior of the different regioisomers, ground state optical properties were computed using density functional theory (DFT) and its time-dependent component (TD-DFT). The CAM-B3LYP/6-31+G(d) level of theory was used along with an implicit solvation model, either chloroform or dichloromethane depending on the considered compound. This protocol has already been used previously on similar molecules[36–38]. Further details about the computational approach are provided in the SI.

Table 2 Experimental (λ_{abs}, nm) and calculated (λ_{calc}, nm) absorption maxima for each regioisomer of **4**, **7**, and **8**. The absolute energy difference between experimental and calculated λ (|ΔE|, in eV), the attribution and the description of the transition, the corresponding oscillator strength (*f*), the charge-transfer distance (d_{CT}, in Å), amount of transferred electron (q_{CT}, in |e|), and the norm of transition dipole moment, ($\|\vec{\mu}_{CT}\|$, in D), have also been reported for each transition.

Compound	λ_{abs}	λ_{calc}	|ΔE|	Attribution	Description	*f*	d_{CT}	q_{CT}	$\|\|\vec{\mu}_{CT}\|\|$
1,6-4	520	522	0.01	$S_0 \rightarrow S_1$	H → L	0.90	0.71	0.40	1.36
1,7-4	518	524	0.03	$S_0 \rightarrow S_1$	H → L	0.86	0.18	0.39	0.35
1,6-7	587	553	0.13	$S_0 \rightarrow S_1$	H → L	0.90	0.72	0.47	1.60
1,7-7	616	577	0.14	$S_0 \rightarrow S_1$	H → L	0.85	0.30	0.46	0.66
1,6-8	389	394	0.04	$S_0 \rightarrow S_3$	H → L+1	2.58	0.21	0.54	0.54
1,7-8	373	374	0.01	$S_0 \rightarrow S_3$	H-2 → L	2.36	0.12	0.54	0.31

After an optimization step, the optical properties, and especially the main absorption peak (λ_{abs} and λ_{calc}), of the two regioisomers of **4**, **7**, and **8** were computed and compared to the experimental ones (**Table 2**). The difference between the calculated and the experimental λ are systematically lower than the traditional accuracy threshold of 0.2 eV, indicating an adequate computational approach. Beyond the reproduction of the main absorption peak for each regioisomer, it has also been possible to retrieve quantitatively the difference between regioisomers (red-shift for **1,7-7** compared to **1,6-7**, blue-shift for **1,7-8** compared to **1,6-8** and no significant modification between **1,6-4** and **1,7-4**) and to reproduce nicely the shape of the different spectra (**Figure S29**).

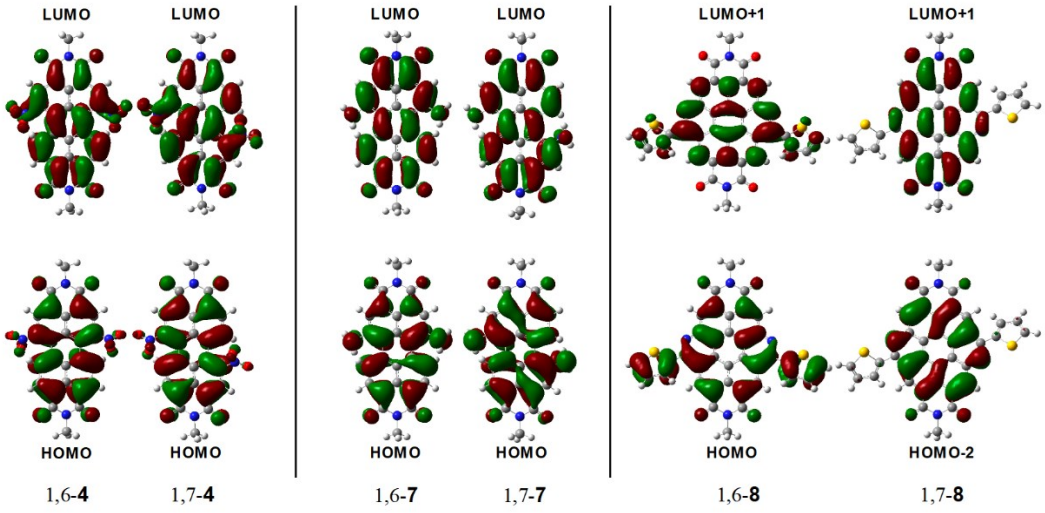

Fig. 7 Representation of the most important molecular orbitals corresponding to λ_{calc} for each regioisomer of **4**, **7** and **8**. Isodensity=0.0004 a.u.

For **4** and **7** the main absorption peak corresponds to a $S_0 \rightarrow S_1$ excitation and is described by HOMO-LUMO transition (**Table 2** and **Figure 7**). For **8**, the main absorption peak ascribes to a $S_0 \rightarrow S_3$ excitation, mainly described by HOMO-LUMO+1 (**1,6-8**) and HOMO−2-LUMO (**1,7-8**) transitions and by HOMO-LUMO transitions in a lesser extent for both molecules (**Figure S28**). All the orbitals that are involved are localized on the conjugated core of the molecules, corresponding to π-π* transitions, reinforcing the choice of not considering the alkyl lateral chains (**Table S2**). The charge transfer (CT) character was also investigated. Due to the symmetry of the molecules, especially the 1,7 regioisomers, all the descriptors (d_{CT}, q_{CT} and $||\vec{\mu}_{CT}||$) have low values. It is due to the fact that the transitions are localized only on the perylene core. The representation of the transition electronic density variation (**Figure S30**) and of $\vec{\mu}_{CT}$ (**Figure S31**) are gathered in the SI. It is worth noticing that the *bay*-substituents are always involved in the main absorption band and can thus be tuned to modify the absorption spectra of the molecules.

Conclusion

We developed an efficient regioselective synthetic strategy to prepare 1,6/7-$(NO_2)_2$PDI and 1,6/7-$(NH_2)_2$PDI on large scales. Not only these derivatives can be engaged into similar reactions as their halogenated equivalents such as S_NAr, Pd-catalysed couplings, hetero-annulations, reductions and more, but they represent the only example of bis-*bay*-substituted PDIs available as pure 1,6 and 1,7 regioisomers. The well-noticeable differences in optical and electronic properties measured here for each regioisomers highlight the importance of this work, as they should afford different performances and characteristics in devices. This combination of unique advantages makes these nitro and amino derivatives highly attracting building blocks for the development of new n-type materials for organic electronics.

Conflicts of interest

There are no conflicts to declare

Acknowledgements

The authors acknowledge the Université d'Angers and SFR MATRIX for the access to the CARMA platform, Dr. Ingrid Freuze for Mass Spectrometry measurements, Benjamin Siegler for NMR experiments. L. L. B thanks the supercomputer facilities of the Mésocentre de calcul de Franche-Comté. This work received support from the "Etoiles Montantes" funding scheme (A. G., project CURVY, 2021_11614) funded by the PULSAR 2021 program from the Région Pays de la Loire and the Université d'Angers, and the Agence Nationale de la Recherche (A. G., PhotoSynth ANR JCJC 2021, ANR-21-CE06-0015-01).

Notes and references

1 W. Jiang and Z. Wang, Molecular Carbon Imides, *J. Am. Chem. Soc.*, 2022, **144**, 14976–14991.
2 A. Nowak-Król, K. Shoyama, M. Stolte and F. Würthner, Naphthalene and perylene diimides – better alternatives to fullerenes for organic electronics?, *Chem. Commun.*, 2018, **54**, 13763–13772.

3 M. Li, H. Yin and G.-Y. Sun, PDI derivatives with functional active position as non-fullerene small molecule acceptors in organic solar cells: From different core linker to various conformation, *Appl. Mater. Today*, 2020, **21**, 100799.
4 V. Sharma, J. D. B. Koenig and G. C. Welch, Perylene diimide based non-fullerene acceptors: top performers and an emerging class featuring N-annulation, *J. Mater. Chem. A*, 2021, **9**, 6775–6789.
5 Z. Li, D. Yang, X. Zhao, Z. Li, T. Zhang, F. Wu and X. Yang, New PDI-based small-molecule cathode interlayer material with strong electron extracting ability for polymer solar cells, *RSC Adv.*, 2016, **6**, 101645–101651.
6 J. Li, P. Li, M. Fan, X. Zheng, J. Guan and M. Yin, Chirality of Perylene Diimides: Design Strategies and Applications, *Angew. Chem. Int. Ed.*, 2022, **61**, e202202532.
7 A. Nowak-Król and F. Würthner, Progress in the synthesis of perylene bisimide dyes, *Org. Chem. Front.*, 2019, **6**, 1272–1318.
8 Q. Shi, J. Wu, X. Wu, A. Peng and H. Huang, Perylene Diimide-Based Conjugated Polymers for All-Polymer Solar Cells, *Chem. – Eur. J.*, 2020, **26**, 12510–12522.
9 L. Chen, C. Li and K. Müllen, Beyond perylene diimides: synthesis, assembly and function of higher rylene chromophores, *J Mater Chem C*, 2014, **2**, 1938–1956.
10 R. K. Dubey, A. Efimov and H. Lemmetyinen, 1,7- And 1,6-Regioisomers of Diphenoxy and Dipyrrolidinyl Substituted Perylene Diimides: Synthesis, Separation, Characterization, and Comparison of Electrochemical and Optical Properties, *Chem. Mater.*, 2011, **23**, 778–788.
11 S. Sengupta, R. K. Dubey, R. W. M. Hoek, S. P. P. van Eeden, D. D. Gunbaş, F. C. Grozema, E. J. R. Sudhölter and W. F. Jager, Synthesis of Regioisomerically Pure 1,7-Dibromoperylene-3,4,9,10-tetracarboxylic Acid Derivatives, *J. Org. Chem.*, 2014, **79**, 6655–6662.
12 G. Shao, M. Wu, X. Wang, J. Zhao, X. You, D. Wu and J. Xia, Regiochemically Pure 1,6-Ditriflato-Perylene Diimide: Preparation and Transformation, *J. Org. Chem.*, 2022, **87**, 14825–14832.
13 Y. Liu, Y. Wang, L. Ai, Z. Liu, X. Ouyang and Z. Ge, Perylenebisimide regioisomers: Effect of substituent position on their spectroscopic, electrochemical, and photovoltaic properties, *Dyes Pigments*, 2015, **121**, 363–371.
14 P. Simón Marqués, F. Tintori, J. M. Andrés Castán, P. Josse, C. Dalinot, M. Allain, G. Welch, P. Blanchard and C. Cabanetos, Indeno[1,2-b]thiophene End-capped Perylene Diimide: Should the 1,6-Regioisomers be systematically considered as a byproduct?, *Sci. Rep.*, 2020, **10**, 3262.
15 L. Rocard, A. Goujon and P. Hudhomme, Nitro-Perylenediimide: An Emerging Building Block for the Synthesis of Functional Organic Materials, *Molecules*, 2020, **25**, 1402.
16 R. El-Berjawi and P. Hudhomme, Synthesis of a perylenediimide-fullerene C60 dyad: A simple use of a nitro leaving group for a Suzuki-Miyaura coupling reaction, *Dyes Pigments*, 2018, **159**, 551–556.
17 M. Hruzd, L. Rocard, A. Goujon, M. Allain, T. Cauchy and P. Hudhomme, Desymmetrization of Perylenediimide Bay Regions Using Selective Suzuki–Miyaura Reactions from Dinitro Substituted Derivatives, *Chem. – Eur. J.*, 2020, **26**, 15881–15891.
18 A. Makhloutah, D. Hatych, T. Chartier, L. Rocard, A. Goujon, F.-X. Felpin and P. Hudhomme, An investigation of palladium-catalyzed Stille-type cross-coupling of nitroarenes in perylenediimide series, *Org. Biomol. Chem.*, 2022, **20**, 362–365.
19 M. Schulze, M. Philipp, W. Waigel, D. Schmidt and F. Würthner, Library of Azabenz-Annulated Core-Extended Perylene Derivatives with Diverse Substitution Patterns and Tunable Electronic and Optical Properties, *J. Org. Chem.*, 2016, **81**, 8394–8405.
20 M. Schulze, A. Steffen and F. Würthner, Near-IR Phosphorescent Ruthenium(II) and Iridium(III) Perylene Bisimide Metal Complexes, *Angew. Chem. Int. Ed.*, 2015, **54**, 1570–1573.
21 L. Hao, W. Jiang and Z. Wang, Integration of nitrogen into coronene bisimides, *Tetrahedron*, 2012, **68**, 9234–9239.
22 A. Goujon, L. Rocard, H. Melville, T. Cauchy, C. Cabanetos, S. Dabos-Seignon and P. Hudhomme, bay-Dissymmetrical hetero- and Aza-Benzannulated PeryleneDiimides as new n-type semiconductors, *J. Mater. Chem. C*, 2022, **10**, 14939–14945.
23 H. Sun, Z. Mu, C. Yang, K. Zhang, X. Ji, T. Zhang, H. Ding, S. Wang, L. Dong, J. Zhang and Q. Zhang, Facile Azabenz-Annulations through UV-induced Photocyclization: A Promising Method for Perylenediimide-Based Organic Semiconductors, *Chem. – Asian J.*, 2022, **17**, e202101323.
24 H. Sun, J. Jin, Q. Wang, S. Wang, W. Na, Z. Li, B. Yao, P. Sun, L. Dong and X.-C. Hang, An azabenz-annulated perylenediimide with tetraphenylethene units: Aggregation-induced emission, mechanochromic fluorescence, and cell imaging, *Dyes Pigments*, 2022, **200**, 110169.
25 A. Makhloutah, A. Hoff, A. Goujon, G. C. Welch and P. Hudhomme, AzaBenzannulated perylene diimide multimers as electron acceptors for organic solar cells, *Mater. Chem. Front.*, 2022, **6**, 3237–3242.
26 H.-Y. Tsai and K.-Y. Chen, Synthesis and optical properties of novel asymmetric perylene bisimides, *J. Lumin.*, 2014, **149**, 103–111.

27 K.-Y. Chen and T. J. Chow, 1,7-Dinitroperylene bisimides: facile synthesis and characterization as n-type organic semiconductors, *Tetrahedron Lett.*, 2010, **51**, 5959–5963.
28 H.-Y. Tsai and K.-Y. Chen, 1,7-Diaminoperylene bisimides: Synthesis, optical and electrochemical properties, *Dyes Pigments*, 2013, **96**, 319–327.
29 H.-Y. Tsai, C.-W. Chang and K.-Y. Chen, 1,6- and 1,7-regioisomers of dinitro- and diamino-substituted perylene bisimides: synthesis, photophysical and electrochemical properties, *Tetrahedron Lett.*, 2014, **55**, 884–888.
30 Y. Zhang, Z. Zhao, X. Huang, Y. Xie, C. Liu, J. Li, X. Guan, K. Zhang, C. Cheng and Y. Xiao, N-type organic semiconductor bisazacoronene diimides efficiently synthesized by a new type of photocyclization involving a Schiff base, *RSC Adv.*, 2012, **2**, 12644.
31 P. J. Amal Joseph, S. Priyadarshini, M. Lakshmi Kantam and H. Maheswaran, Copper catalyzed ipso-nitration of iodoarenes, bromoarenes and heterocyclic haloarenes under ligand-free conditions, *Tetrahedron Lett.*, 2012, **53**, 1511–1513.
32 S. Saito and Y. Koizumi, Copper-catalyzed coupling of aryl halides and nitrite salts: a mild Ullmann-type synthesis of aromatic nitro compounds, *Tetrahedron Lett.*, 2005, **46**, 4715–4717.
33 Paik, Seung-Uk and Jung, Myoung-Geun, Rapid Microwave-Assisted Copper-Catalyzed Nitration of Aromatic Halides with Nitrite Salts, *Bull. Korean Chem. Soc.*, 2012, **33**, 689–691.
34 G.-A. Lee, H.-C. Lin, H.-Y. Lee, C.-H. Chen and H.-Y. Huang, Ipso Nitration of 2-Halothiophenes with Silver Nitrate, *Asian J. Org. Chem.*, 2017, **6**, 1733–1736.
35 A. Goujon, L. Rocard, T. Cauchy and P. Hudhomme, An Imine Photocyclization as an Alternative to the Pictet–Spengler Reaction for the Synthesis of AzaBenzannulated Perylenediimide Dyes, *J. Org. Chem.*, 2020, **85**, 7218–7224.
36 E. P. Farr, M. T. Fontana, C.-C. Zho, P. Wu, Y. L. Li, N. Knutson, Y. Rubin and B. J. Schwartz, Bay-Linked Perylenediimides are Two Molecules in One: Insights from Ultrafast Spectroscopy, Temperature Dependence, and Time-Dependent Density Functional Theory Calculations, *J. Phys. Chem. C*, 2019, **123**, 2127–2138.
37 D. Aranda, N. J. Schuster, X. Xiao, F. J. Ávila Ferrer, F. Santoro and C. Nuckolls, Origin of Chiroptic Amplification in Perylene-Diimide Helicenes, *J. Phys. Chem. C*, 2021, **125**, 2554–2564.
38 S. R. Bora and D. J. Kalita, Hopping transport in perylene diimide based organic solar cells: a DFT approach, *New J. Chem.*, 2022, **46**, 19357–19372.

Graphical Abstract